Sialic acid as a biomarker studied in breast cancer cells using fluorescent molecularly imprinted polymers, MIPs

Zahra El-Schich
Malmo Universitet
Yuecheng Zhang
Malmo Universitet
Tommy Göransson
Skanes universitetssjukhus Lund
Nishtman Dizeyi
Lunds Universitet
Jenny Persson
Umea Universitet Medicinska fakulteten
Emil Johansson
Umea Universitet Teknisk-Naturvetenskaplig Fakultet
Remi Caraballo
Umea Universitet Teknisk-Naturvetenskaplig Fakultet
Mikael Elofsson
Umea Universitet Teknisk-Naturvetenskaplig Fakultet
Sudhirkumar Shinde
Central Queensland University School of Engineering and Technology
Börje Sellergren
Malmo Universitet
Anette Gjörloff Wingren (anette.gjorloff-wingren@mau.se)
Malmo Universitet https://orcid.org/0000-0002-2993-0354
Nishtman Dizeyi
Cernelle

Research

Keywords: cancer, CD44, EpCAM, Glycan, Lectin, Molecularly imprinted polymers, Sialic acid

Posted Date: May 10th, 2020

DOI: https://doi.org/10.21203/rs.3.rs-26744/v1

Sialic acid as a biomarker studied in breast cancer cells using fluorescent molecularly imprinted polymers, MIPs

Zahra El-Schich[1,2], Yuecheng Zhang[1,2], Tommy Göransson[1], Nishtman Dizeyi[3], Jenny L. Persson[1,2,4], Emil Johansson[5], Remi Caraballo[5], Mikael Elofsson[5], Sudhir Shinde[6], Börje Sellergren[1,2], Anette Gjörloff Wingren[1,2]

1) Department of Biomedical Sciences, Faculty of Health and Society, Malmö University, Malmö, Sweden
2) Biofilms-Research Center for Biointerfaces, Malmö University, Malmö, Sweden
3) Department of Translational Medicine, Lund University, Malmö, Sweden
4) Department of Molecular Biology, Umeå University, Umeå, Sweden
5) Department of Chemistry, Umeå University, Umeå, Sweden, and Umeå Centre for Microbial Research, Umeå University, Umeå, Sweden
6) School of Chemistry and Chemical Engineering, Queen´s University, Belfast, UK

Corresponding author: Anette Gjörloff Wingren, Department of Biomedical Sciences, Faculty of Health and Society, Malmö University, Malmö, Sweden. E-mail: anette.gjorloff-wingren@mau.se

Abstract

Sialylations are post-translational modifications of proteins and lipids that play important roles in many cellular events, including cell-cell interactions, proliferation and migration. Tumor cells express high levels of sialic acid (SA), which are often associated with the increased invasive potential in clinical tumors correlating with poor prognosis. To overcome the lack of natural SA-receptors, such as antibodies and lectins with high enough specificity and sensitivity, we have used molecularly imprinted polymers (MIPs), or "plastic antibodies", as nanoprobes. Since high expression of EpCAM in primary tumors often is associated with proliferation and a more aggressive phenotype, the expression and of epithelial cell adhesion molecule (EpCAM) CD44 was initially analyzed. The SA-MIPs were used here for the detection of SA on the cell surface of breast cancer cells. Lectins that specifically bind to the α-2,3 SA and α-2,6 SA variants, respectively, were used for analysis of SA expression with both flow cytometry and confocal microscopy. Here we show a correlation of EpCAM and SA expression when using the SA-MIPs for detection of SA. We also demonstrate the binding pattern of the SA-MIPs on the breast cancer cell lines using confocal microscopy. Pre-incubation of the SA-MIPs with SA-derivatives as inhibitors could reduce the binding of the SA-MIPs to the tumor cells, indicating the specificity of the SA-MIPs. In conclusion, the SA-MIPs may be a new powerful tool in the SA-analysis of breast cancer cells.

Keywords: Breast cancer, CD44, EpCAM, Glycan, Lectin, Molecularly imprinted polymers, Sialic acid.

Introduction

Breast cancer is a complex and highly heterogeneous disease, and the most commonly diagnosed cancer in women worldwide. Despite recent improvements in overall survival rates, it is still the second leading cause of mortality due to cancer in women (1). Different classification categories of breast cancer comprise luminal A, luminal B, basal-like, human epidermal growth factor receptor 2 (HER2)-positive and normal subgroups (2). Twenty years ago, the development of molecular profiling using DNA microarrays proved this heterogeneity, demonstrated through gene expression profiling and immunohistochemical expression (3).

During tumor growth, cancer cells can be detected and eliminated by the immune system, but some cancer cells may exploit several mechanisms to evade destruction by the immune system, enabling them to escape immune surveillance and progress through the metastatic cascade (4). The circulating cancer cells released from primary tumors (CTCs) are considered to have capability to initiate distant metastasis. Detection and isolation of CTCs using the Food and Drug Administration (FDA)-approved CellSearch platform is based on an automated immunomagnetic sorting and on expression of the epithelial cell adhesion molecule (EpCAM) and cytokeratin (CK) (5). High expression of EpCAM in primary tumors is often associated with proliferation and a more aggressive phenotype with respect to overall survival and appearance of metastasis (6). The inadequacy of EpCAM as universal marker for CTCs detection seems unquestionable and alternative methods able to recognize a broader spectrum of phenotypes are definitely needed (7).

Alterations in protein glycosylation contribute to malignant transformation and cancer progression (8). Sialic acid (SA), or 5-N-acetylneuraminic acid (Neu5Ac), is a monosaccharide that plays an important role in a variety of biological processes in the cells (9). SA is chemically bound to galactose (Gal) or N-acetylgalactosamine (GalNAc) and the underlying glycan via α-2,3 or α-2,6 glycosidic linkage (9). Increased levels of SA on tumor cells are often associated with the increased invasive potential in clinical tumors correlating with poor prognosis (10). High SA expression also favors cancer metastasis by facilitating cancer cell detachment and protection from detachment-induced apoptosis, enhancing migration and tissue invasion by increasing integrin interactions with the extra cellular matrix (ECM), preventing immune recognition and eradication and enabling interactions with

endothelial cells to extravasate from the bloodstream and form metastases (11). Upon malignant transformation, cancer cells upregulate sialyltransferase expression resulting in the accumulation of sialoglycans on their surface (12, 13). Previously, we have shown the usage of fluorescent SA-MIP nanoprobes for detection of SA on cancer cells such as DU145, PC-3, Jurkat and B-CLL and further verified the binding specificity by enzymatic cleavage (14, 15).

Available lectins and glycan specific antibodies for detection of SA containing glycoconjugates do not perform well in e.g. analytics of glycoproteomes and appropriate high-throughput cellular imaging technologies (16). Therefore, the studies by us and others are of high importance to develop novel tools for glycan detection. Wang et al imprinted fluorescent monosaccharide MIPs against SA, fucose and mannose by using boronic acid functionality and sol-gel based surface imprinting approach. The results showed that the nanoprobes exhibited desirable binding properties and could specifically target cancer cells over normal cells (17). Using an innovative multilayered core-shell architecture comprising quantum dot cores, nanoprobes were developed for selective targeting and imaging of hyaluronan and sialylated glycosylation sites on human keratinocytes (18).

In the present study, we have performed screening of SA expression on a collection of breast cancer cell lines by using SA-MIPs and lectins, and analyzed interactions by flow cytometry and confocal fluorescence microscopy. The breast cancer cell lines were also analyzed using antibodies for the expression of the epithelial EpCAM and the mesenchymal CD44 biomarkers. We show that the SA-MIPs recognize breast cancer cells with low CD44 and high EpCAM expression. The fluorescence microscopy images revealed the staining pattern of both lectins and SA-MIPs. Importantly, by pre-treating the SA-MIPs with SA-derivatives as inhibitors before cell staining, we could demonstrate a concentration-dependent reduction in binding of the SA-MIPs to breast cancer cells as analyzed with flow cytometry.

Materials and methods

Cell culture

Human breast cancer cell lines T47D, MCF-7, Cama-1, MDAMB-468, MDAMB-231 and Hs-578T were obtained from American Type Culture Collection (ATCC/LGC Standards, Teddington, UK). T47D and MCF-7 cells were cultured in RPMI-1640 medium supplemented with 10 % fetal bovine serum and 50 µg/mL gentamycin. MDAMB468 and MDAMB231 cells were cultured in Dulbecco´s Modified Eagle Medium (DMEM) supplemented with 10 % FBS. Cama-1 cells was cultured in RPMI-1640 medium supplemented with 10 % FBS, 1 % pyruvate sodium (Invitrogen) and 1 % penicillin streptomycin. Hs-578T cells was cultured in DMEM supplemented with 10% FBS, 1 % penicillin streptomycin and 10 ug/mL insulin (Sigma-Aldrich, St Louis, USA). The cell lines were incubated in 37 °C with 5 % CO_2 in 100 % humidity. All cell culture reagents except for insulin were from Thermo Fisher Scientific, Waltham, USA).

Flow cytometry analysis

EpCAM staining: $1x10^6$ cells/sample were stained with anti-EpCAM-PE (Milentyi Biotec GmBH, Bergisch Gladbach, Germany) or left unstained as a control. The cells were washed twice with 2 ml PBS. 100 µL of anti-EpCAM-PE with concentrations of 1, 0,5 and 0,25 µg/mL respectively, was added to the cells and 100 µL of PBS was used as a negative control. The cells were incubated with EpCAM-PE for 30 min at 4 °C in dark, were thereafter washed three times with 2 ml PBS, and analyzed using flow cytometry (BD Biosciences, Accuri C6 Flow Cytometry, NJ).

CD44 staining: $1x10^6$ cells/sample were stained with human anti-CD44 antibody (R&D, Minneapolis, MN, USA) or left unstained as a control. The cells were washed twice with 2 ml PBS. 100 µL of anti-CD44 with concentration 2,5 µg/mL was added to the cells and 100 µL of PBS was used as a negative control and incubated for 30 min at 4 ºC in dark. After incubation the cells were washed twice with 2 mL PBS. Anti-rat-FITC (R&D) were used as a secondary antibody. 100 µL of 1/10 diluted anti-rat-FITC was added to the cells and to the negative control. The cells were incubated for 30 min at 4 °C in dark, were thereafter washed three times with 2 ml PBS, and analyzed using flow cytometry.

MAL I and SNA *(Lectin-Biotin)*: $1x10^6$ cells/sample were stained with Lectin-Biotin (Vector Laboratories, Burlingame, CA, USA) both for MAL I and SNA or left unstained as a control. The cells were washed twice with 2 ml phosphate buffered saline (PBS, Thermo Fischer

Scientific). 100 µL of Lectin-Biotin with concentrations of 2, 1 and 0,5 µg/mL respectively, was added to the cells and 100 µL of PBS was used as a negative control. The cells were incubated with Lectin-Biotin for 30 min on 4 °C and were thereafter washed three times with 2 ml PBS. Thereafter 100 µL of 1:100 dilutions of streptavidin-FITC (Sigma) was added to the cells and incubated for 20 min at 4 °C in dark. After the incubation, the cells were washed three times with 2 mL PBS and analyzed using flow cytometry.

SA-MIPs: $1x10^6$ cells/sample were stained with SA-MIPs or left unstained as a control. The cells were washed twice with 2 ml PBS. 100 µL of SA-MIPs with concentration of 0,1 mg/mL was added to the cells and 100 µL of PBS was used as a negative control. The cells were incubated with SA-MIP for 30 min at 4°C and were thereafter washed three times with 2 ml PBS and analyzed using flow cytometry.

Fluorescence microscopy

$5x10^4$ cells/samples were adhered to poly-lysine slides (Thermo Fisher Scientific) in a 6 wells plate for 2 h, at 37 °C with 5 % CO_2 in 100 % humidity. After the incubation, 2 mL cell culture medium was added to the wells and incubated for 48 h. After the incubation, the cells were washed three times with PBS and fixed with 100 µl 4 % formaldehyde for 10 min, followed with three times wash with PBS. After permeabilization with 0,05 % TritonX (Sigma) the cells were incubated with rhodamine-Phalloidin (Sigma) for 30 min in dark at RT. After two more wash with 0,05 % Triton-X and PBS, the cells were incubated with 100 µl of SA-MIPs (0,1 mg/mL) or biotinylated MAL I and SNA, 10 µg/ml) for 30 min at RT. The biotinylated lectins were further incubated with streptavidin-FITC. After the incubation, the cells were washed four times with PBS and incubated with 100 µl 300 nM DAPI (Thermo Fisher Scientific) in PBS, for 4 min at RT. After three more washes with PBS, the cells were mounted with one drop of mounting medium Prolong® Gold antifade reagent (Molecular probes).

Pre-treatment of SA-MIPs with SA- derivatives: The cells were harvested and washed twice with 2 ml PBS. SA-MIPs and two different SA-derivatives (ME0970 and ME1057) (19) at either 20 uM or 200 uM in 100 µL were pre-incubated in PBS for 5 min before added to $1x10^6$ cells/sample or left unstained as a control. In addition, 100 µL of SA-MIPs with concentration of 0,1 mg/mL was used as a positive staining control. The cells were incubated for 30 min at 4°C and were thereafter washed three times with 2 ml PBS and analyzed using flow cytometry.

Results

Expression of EpCAM and CD44 on breast cancer cell lines

The expression levels of EpCAM were analyzed in the six different breast cancer cell lines. Hs-578T and MDAMB231 expressed EpCAM at low levels compared to MDAMB468, T47D, Cama-1 and MCF-7, which express EpCAM at higher levels (Figure 1a). For CD44 expression, the Hs-578T, MDAMB231 and MDAMB468 express CD44at high levels compared to T47D, Cama-1 and MCF-7, which express CD44 at lower levels (Figure 1b).

SA staining with lectins on breast cancer cell lines

In this study, two different lectins were used and analyzed by flow cytometry and fluorescence microscopy. MAL I appear to bind carbohydrate structures that contain SA attached to terminal galactose in α-2,3 linkage. The 2,3-SA expression is presented in figure 2A. T47D, MDAMB231 and MCF-7 expressed high α-2,3 linkage levels compared to Cama-1 and Hs-578T, which express low levels of α-2,3 linkage, as determined by the mean fluorescence intensity (MFI). SNA binds preferentially to SA attached to terminal galactose in α-2,6 and to a lesser degree, α-2,3 linkage (ref). The 2,6-SA expression is presented in figure 2B. T47D and MDAMB468 showed highest α-2,6 linkage levels compared to MCF-7 and Hs-578T, which showed low levels of α-2,6 linkage. The fluorescent microscopy results correlate well with the flow cytometry results (Fig 3).

SA staining with SA-MIPs on breast cancer cell lines

The expression levels for SA was analyzed using SA-MIPs and flow cytometry in six different breast cancer cell lines. According to the binding pattern, Hs-578T and MDAMB231 expressed SA at low levels compared to MDAMB468, T47D, Cama-1 and MCF-7, which expressed SA at higher levels. Interestingly, the results indicate that low EpCAM expression levels correlate with low SA expression levels (Figure 4). Also, there is an inverse correlation between SA- and CD44-expression.

In order to visualize the surface binding of SA, breast cancer cell lines were stained with SA-MIPs and analyzed with fluorescent microscopy. In figure 5, the membrane staining of the breast cancer cell lines using SA-MIPs, actin filament staining with phalloidin and nuclei staining using DAPI is shown.

Pre-treatment of SA-MIPs with SA-derivative reduce the binding to cells

The SA-derivates ME0970 or ME1057 were pre-incubated at either 20 uM or 200 uM, respectively, with 0,1 mg/ml SA-MIPs and then added to the T47D cells. The binding of the pre-treated cells was compared with the binding to the same cell line of 0,1 mg/ml of SA-MIPs alone, and was shown to be reduced with 7% (20 uM) and 66% (200 uM), respectively, for ME0970, and with 0,5% (20 uM) and 64% (200 uM), respectively, for ME1057 (Figure 6). The reduction in binding of the pre-treated cells was concentration-dependent, as shown with both SA conjugates.

Discussion

Glycosylation is the most abundant post-translational modification and the majority of eukaryotic cells express cell surface glycans (20). The knowledge about the glycome has increased in the past years. Indeed, the role of glycans in cancer have been highlighted by the fact that alterations in glycosylation regulate the development and progression of cancer. Thus, glycans serve as important biomarkers. We have developed SA-imprinted fluorescent nanoprobes to enable SA-detection, for the use as novel tools in cancer diagnostics (14). The correlation of SA-MIP binding and EpCAM expression on the breast cancer cell lines presented in this study show an additive level of phenotyping of breast cancer cells, together with the CD44 biomarker, which showed a reverse correlation. High expression levels of EpCAM in tumors are often associated with proliferation and a more aggressive phenotype with respect to overall survival and appearance of metastasis (6). Identification of EpCAM glycosylation sites or structures may be a crucial step to define the potential role of EpCAM in breast cancer cells (21). Various cancer cells are lacking EpCAM expression, therefore CellSearch approaches are limited (22). Indeed, carcinoma cells undergoing epithelial-to-mesenchymal transition, can at least partially downregulate epithelial cell–specific molecules such as EpCAM (23).

Our results show that breast cancer cells expressing α-2,3 or α-2,6 glycosidic linkage can bind the SA-MIPs to various degrees. The confocal microscopy results show the binding pattern of the SA-MIPs to the different cell types. For flow cytometry analysis, we could characterize the binding pattern of MAL, SNA and SA-MIPs to all six cell lines and showed that the binding of the SA-MIPs to the cell line T47D could be inhibited by addition of two different SA-derivatives. Because of their efficient inhibition ability, SA-derivatives can be used for specificity tests for SA-MIPs. The two SA-derivatives used in this study were designed of multivalent ligands intended for topical administration for the viruses CVA24v and HAdV-37 that utilize SA for cell attachment (19).

Others have shown that SA-imprinted nanoparticles could selectively bind with SA overexpressed in DU145 cancer cells (24). In their hands, DU145 cells, but not HeLa cells bound the SA-imprinted nanoparticles, revealing a specificity in binding. Moreover, unmodified nanoparticles did not show any binding to the two cell lines. Interestingly, Wang et al showed that SA-MIPs could specifically target cancer cells over normal cells, and that

addition of SA could compete out the SA-MIP binding to the cancer cells (17). These results support our observation using the SA derivates, although we cannot completely reduce the binding to SA-expressing cells.

The majority of breast cancers carry Tn (GalNAc-Ser/Thr) within the same cell and in close proximity to extended glycan T (Galβ1,3GalNAc) the addition of Gal to the GalNAc being catalysed by the T synthase (25). In breast cancer, there can also be a change in the number of O-GalNAc glycans added to the peptide core of glycoproteins, as well as changes in the core structures, which often results in increased sialylation. The sialylated derivatives of the O-GalNAc glycans are commonly observed, giving the sialylated Tn (STn) and sialylated core 1 (ST) glycans (20). Truncated mucin-type O-linked glycans are seen often terminating in SA due to up-regulation of sialyltransferases in breast cancers. The altered expression of the sialyltransferase is believed to be the main STn synthase (26). However, novel diagnostic tools with better affinity and specificity are needed. It has been shown that more than 90% of isolated CTCs metastatic bladder and colorectal cancers can overexpress the STn antigen, significantly higher than EpCAM-based detection (27). Recently, Kaptan et al presented the effect of α-2,3 and α-2,6 on cell proliferation, survival and malignant behaviors of thyroid cancer cells. The authors treated the cancer cells with different plant lectins such as MALII, SNA and *Aleuria aurantia lectin* (AAL) (28). These results suggest that altered cell surface glycosylation in cancer seems to be a strong candidate for new therapeutic strategies.

In this study, we provide a discovery strategy in breast cancer cell lines to understand the binding pattern of lectins and MIPs targeting SA.

Conclusions

SA expression correlate with the EpCAM and inversely with CD44 expression levels on a collection of breast cancer cell lines. SA expression could be detected both with SA-MIPs, and the lectins MAL I and SNA. Most interestingly, two different SA-variants could significantly reduce the binding of the SA-MIPs in a concentration-dependent manner. In conclusion, we show a combination of potential biomarkers that can be used to detect epithelial tumor cells that express SA.

Declarations

Ethics approval and consent to participate

Not applicable

Consent for publication

Not applicable

Availability for data and material

All data generated or analysed during this study are included in this published article

Competing interests

The authors declare that they have no competing interests

Funding

This work was supported by grants from the Swedish Knowledge Foundation, the European Union's Horizon 2020 research and innovation program under the Marie Sklodowska-Curie grant agreement No 721297, Biofilms Research Center for Biointerfaces and Malmö University.

Authors´contributions

AGW and ZE conceived and designed the study, ZE, YZ, and TG carried out the cell based studies and performed experiments; SS, EJ and RC synthesized chemical compounds; ZE, BS, ND, JLP, ME, RC and AGW analyzed the data; BS and JLP provided advice and technical assistance; ZE, YZ and AGW wrote the manuscript. All authors read and approved the final manuscript.

Acknowledgements

The authors would like to thank Bo Holmqvist and Anders Brinte at ImaGene-iT, Lund, Sweden, Karin von Wachenfeldt, Truly Translational AB, Sweden, Kersti Alm and Birgit Janicke, PHIAB, Sweden.

Figure legends

1. EpCAM and CD44 expression was analyzed with flow cytometry. Six different breast cancer cell lines were analyzed for EpCAM (a) and CD44 (b) expression pattern. The histograms shows the MFI for each staining including background control.

2. Fluorescence confocal microscopy MAL I - scale bar *20 μm*. Six different breast cancer cell lines were stained for MAL I in green, actin filament in red and nuclear in blue, and analyzed with fluorescence microscopy (a). Fluorescence microscopy SNA- scale bar *10 μm*. Six different breast cancer cell lines were stained for SNA in green, actin filament in red and nuclear in blue, and analyzed with fluorescence confocal microscopy (b).

3. Six breast cancer cell lines were stained with either MAL I or SNA and analyzed with flow cytometry. The histograms shows the MFI for each staining including background control.

4. Fluorescence confocal microscopy SA-MIPs - scale bar *20 μm*. Four different breast cancer cell lines were stained with SA-MIPs in green, rhodamine-phalloidin (actin filaments) in red and DAPI (nuclei) in blue, and analyzed with fluorescence confocal microscopy.

5. EpCAM, CD44 and SA-MIPs analyzed with flow cytometry. Six different breast cancer cell lines were analyzed for EpCAM, CD44 and SA expression pattern. Results are shown in % positive cells.

6. SA-MIPs were pre-incubated with the SA-derivatives ME0970 or ME1057, respectively and analyzed with flow cytometry. The reduction of binding compared to SA-MIP binding alone is shown.

References

1. Howlader NN, Krapcho A. M., et al., editors. SEER Cancer Statistics Review, 1975–2012. Bethesda, MD: National Cancer Institute; 2015.
2. Holliday DL, Speirs V. Choosing the right cell line for breast cancer research. Breast cancer research. 2011;13(4):215.
3. Perou CM, Jeffrey SS, Van De Rijn M, Rees CA, Eisen MB, Ross DT, et al. Distinctive gene expression patterns in human mammary epithelial cells and breast cancers. Proceedings of the National Academy of Sciences. 1999;96(16):9212-7.
4. Zhu L, Narloch JL, Onkar S, Joy M, Broadwater G, Luedke C, et al. Metastatic breast cancers have reduced immune cell recruitment but harbor increased macrophages relative to their matched primary tumors. Journal for immunotherapy of cancer. 2019;7(1):265.
5. Pecot CV, Bischoff FZ, Mayer JA, Wong KL, Pham T, Bottsford-Miller J, et al. A novel platform for detection of CK+ and CK- CTCs. Cancer discovery. 2011;1(7):580-6.
6. van der Gun BTF, Melchers LJ, Ruiters MHJ, de Leij LFMH, McLaughlin PMJ, Rots MG. EpCAM in carcinogenesis: the good, the bad or the ugly. Carcinogenesis. 2010;31(11):1913-21.
7. Raimondi C, Nicolazzo C, Gradilone A. Circulating tumor cells isolation: the "post-EpCAM era". Chinese journal of cancer research = Chung-kuo yen cheng yen chiu. 2015;27(5):461-70.
8. Varki A, Kannagi R, Toole BP. Glycosylation changes in cancer. Essentials of Glycobiology 2nd edition: Cold Spring Harbor Laboratory Press; 2009.
9. Stowell SR, Ju T, Cummings RD. Protein glycosylation in cancer. Annual review of pathology. 2015;10:473-510.
10. Bogenrieder T, Herlyn M. Axis of evil: molecular mechanisms of cancer metastasis. Oncogene. 2003;22(42):6524-36.
11. Büll C, Stoel MA, den Brok MH, Adema GJ. Sialic acids sweeten a tumor's life. Cancer research. 2014;74(12):3199-204.
12. Swindall AF, Londono-Joshi AI, Schultz MJ, Fineberg N, Buchsbaum DJ, Bellis SL. ST6Gal-I protein expression is upregulated in human epithelial tumors and correlates with stem cell markers in normal tissues and colon cancer cell lines. Cancer research. 2013;73(7):2368-78.
13. Harduin-Lepers A, Krzewinski-Recchi MA, Colomb F, Foulquier F, Groux-Degroote S, Delannoy P. Sialyltransferases functions in cancers. Frontiers in bioscience (Elite edition). 2012;4:499-515.
14. Shinde S, El-Schich Z, Malakpour A, Wan W, Dizeyi N, Mohammadi R, et al. Sialic Acid-Imprinted Fluorescent Core–Shell Particles for Selective Labeling of Cell Surface Glycans. Journal of the American Chemical Society. 2015;137(43):13908-12.
15. El-Schich Z, Abdullah M, Shinde S, Dizeyi N, Rosén A, Sellergren B, et al. Different expression levels of glycans on leukemic cells—a novel screening method with molecularly imprinted polymers (MIP) targeting sialic acid. Tumor Biology. 2016:1-6.
16. Loureiro LR, Carrascal MA, Barbas A, Ramalho JS, Novo C, Delannoy P, et al. Challenges in antibody development against Tn and Sialyl-Tn antigens. Biomolecules. 2015;5(3):1783-809.
17. Wang S, Yin D, Wang W, Shen X, Zhu J-J, Chen H-Y, et al. Targeting and imaging of cancer cells via monosaccharide-imprinted fluorescent nanoparticles. Scientific reports. 2016;6:22757.
18. Panagiotopoulou M, Kunath S, Medina-Rangel PX, Haupt K, Bui BTS. Fluorescent molecularly imprinted polymers as plastic antibodies for selective labeling and imaging of hyaluronan and sialic acid on fixed and living cells. Biosensors and Bioelectronics. 2017;88:85-93.
19. Johansson E, Caraballo R, Mistry N, Zocher G, Qian W, Andersson CD, et al. Pentavalent Sialic Acid Conjugates Block Coxsackievirus A24 Variant and Human Adenovirus Type 37–Viruses That Cause Highly Contagious Eye Infections. 2020.
20. Burchell JM, Beatson R, Graham R, Taylor-Papadimitriou J, Tajadura-Ortega V. O-linked mucin-type glycosylation in breast cancer. Biochemical Society transactions. 2018;46(4):779-88.

21. Liu X, Yang L, Zhang D, Liu T, Yan Q, Yang X. Deglycosylation of epithelial cell adhesion molecule affects epithelial to mesenchymal transition in breast cancer cells. Journal of cellular physiology. 2019;234(4):4504-14.
22. Kölbl A, Jeschke U, Andergassen U. The significance of epithelial-to-mesenchymal transition for circulating tumor cells. International journal of molecular sciences. 2016;17(8):1308.
23. Baccelli I, Schneeweiss A, Riethdorf S, Stenzinger A, Schillert A, Vogel V, et al. Identification of a population of blood circulating tumor cells from breast cancer patients that initiates metastasis in a xenograft assay. Nature biotechnology. 2013;31(6):539.
24. Liu R, Cui Q, Wang C, Wang X, Yang Y, Li L. Preparation of sialic acid-imprinted fluorescent conjugated nanoparticles and their application for targeted cancer cell imaging. ACS applied materials & interfaces. 2017;9(3):3006-15.
25. Beatson R, Maurstad G, Picco G, Arulappu A, Coleman J, Wandell HH, et al. The breast cancer-associated glycoforms of MUC1, MUC1-Tn and sialyl-Tn, are expressed in COSMC wild-type cells and bind the C-type lectin MGL. PLoS One. 2015;10(5):e0125994.
26. Marcos NT, Bennett EP, Gomes J, Magalhaes A, Gomes C, David L, et al. ST6GalNAc-I controls expression of sialyl-Tn antigen in gastrointestinal tissues. Front Biosci (Elite Ed). 2011;3(4):1443-55.
27. Neves M, Azevedo R, Lima L, Oliveira MI, Peixoto A, Ferreira D, et al. Exploring sialyl-tn expression in microfluidic-isolated circulating tumour cells: A novel biomarker and an analytical tool for precision oncology applications. New biotechnology. 2019;49:77-87.
28. Kaptan E, Sancar‐Bas S, Sancakli A, Bektas S, Bolkent S. The effect of plant lectins on the survival and malignant behaviors of thyroid cancer cells. Journal of cellular biochemistry. 2018;119(7):6274-87.

Figure 1a

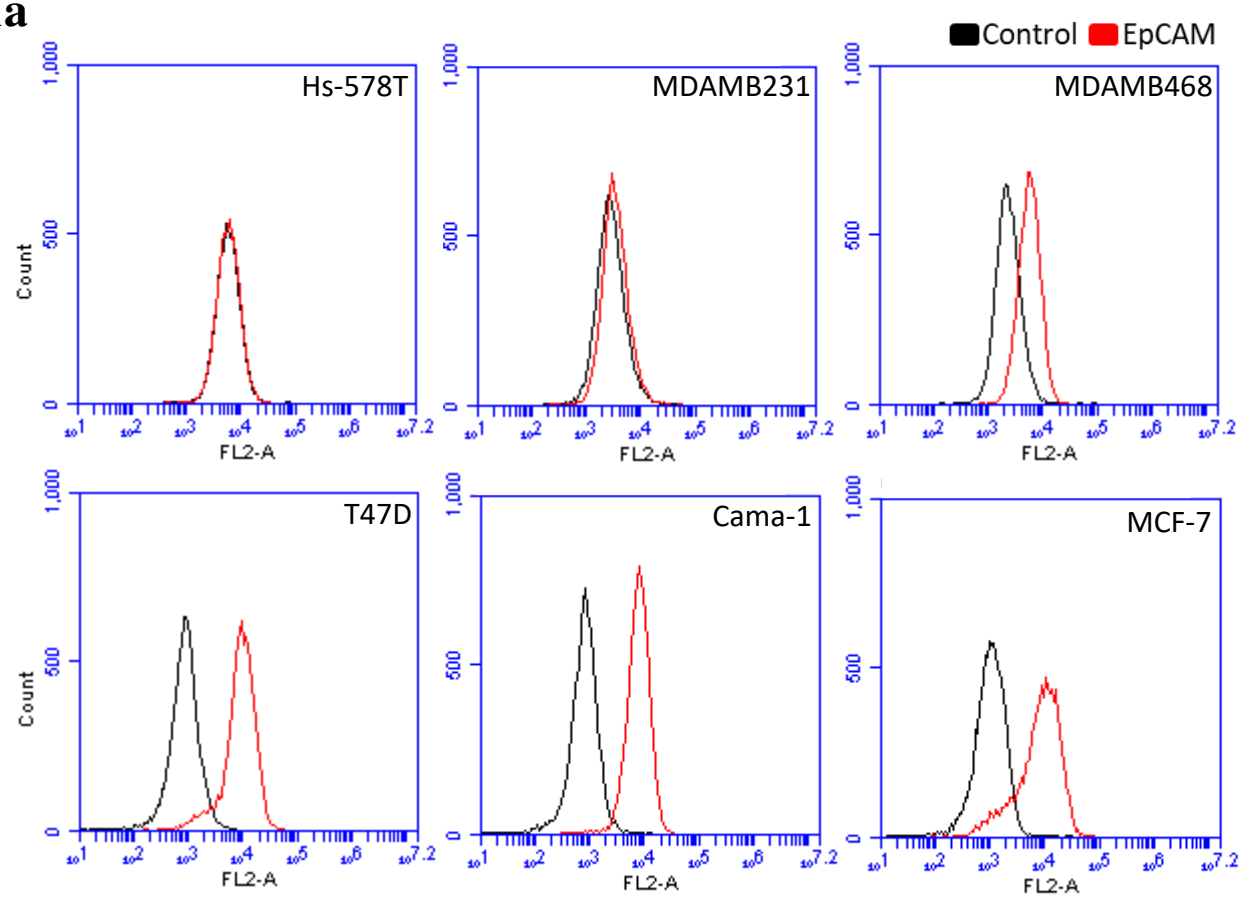
Control
EpCAM
Hs-578T
MDAMB231
MDAMB468
T47D
Cama-1
MCF-7
Count
FL2-A
1,000
500
0

Figure 1b

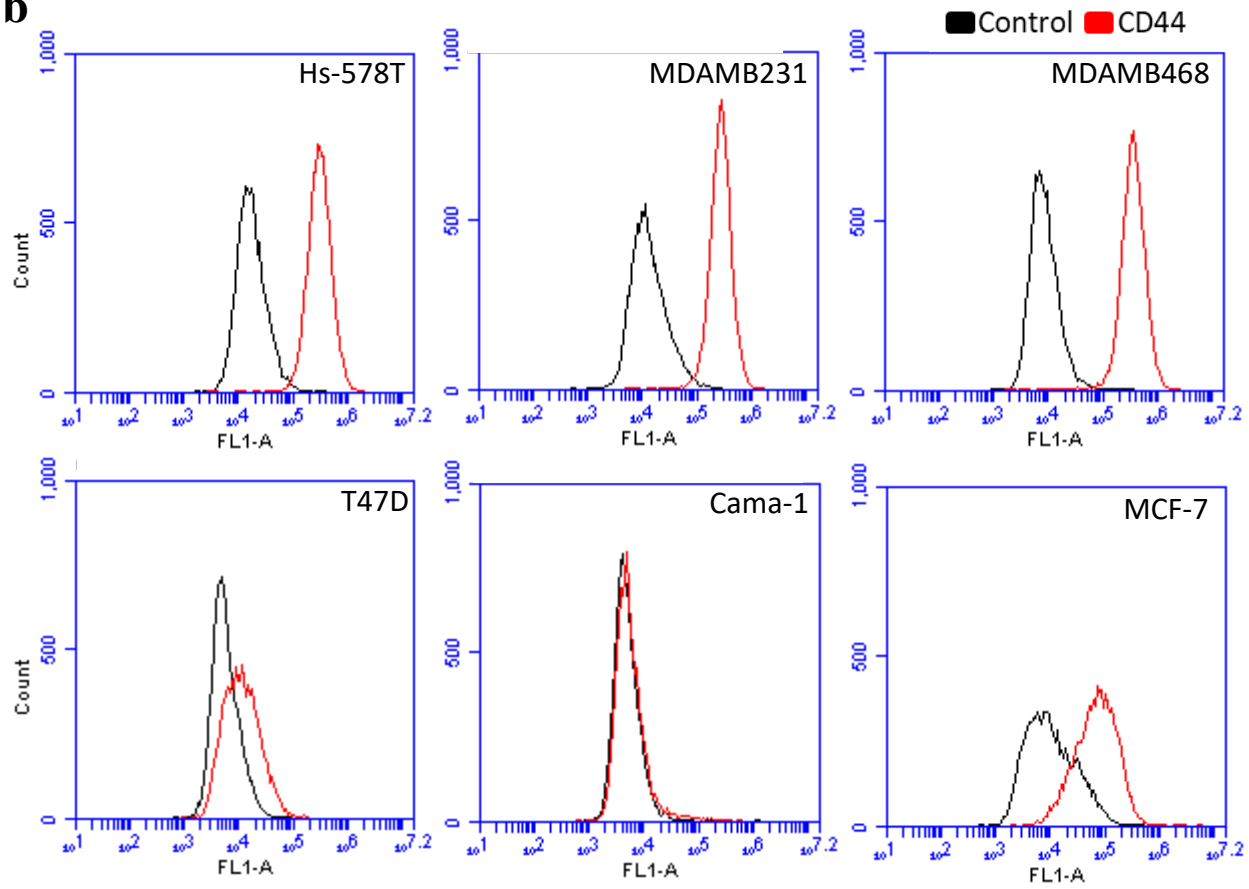
Control
CD44
Hs-578T
MDAMB231
MDAMB468
T47D
Cama-1
MCF-7
Count
FL1-A

Figure 2a

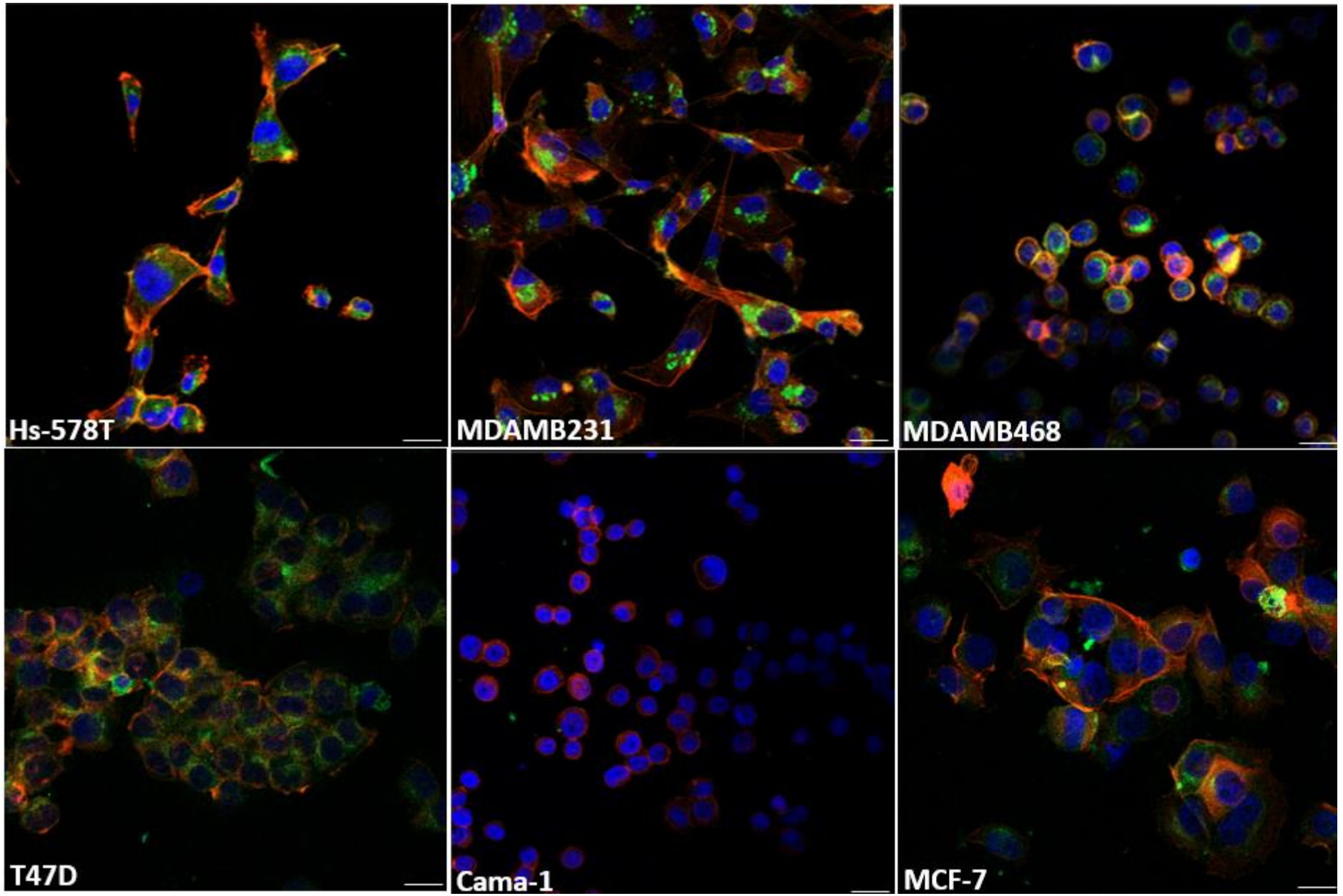

Figure 2b

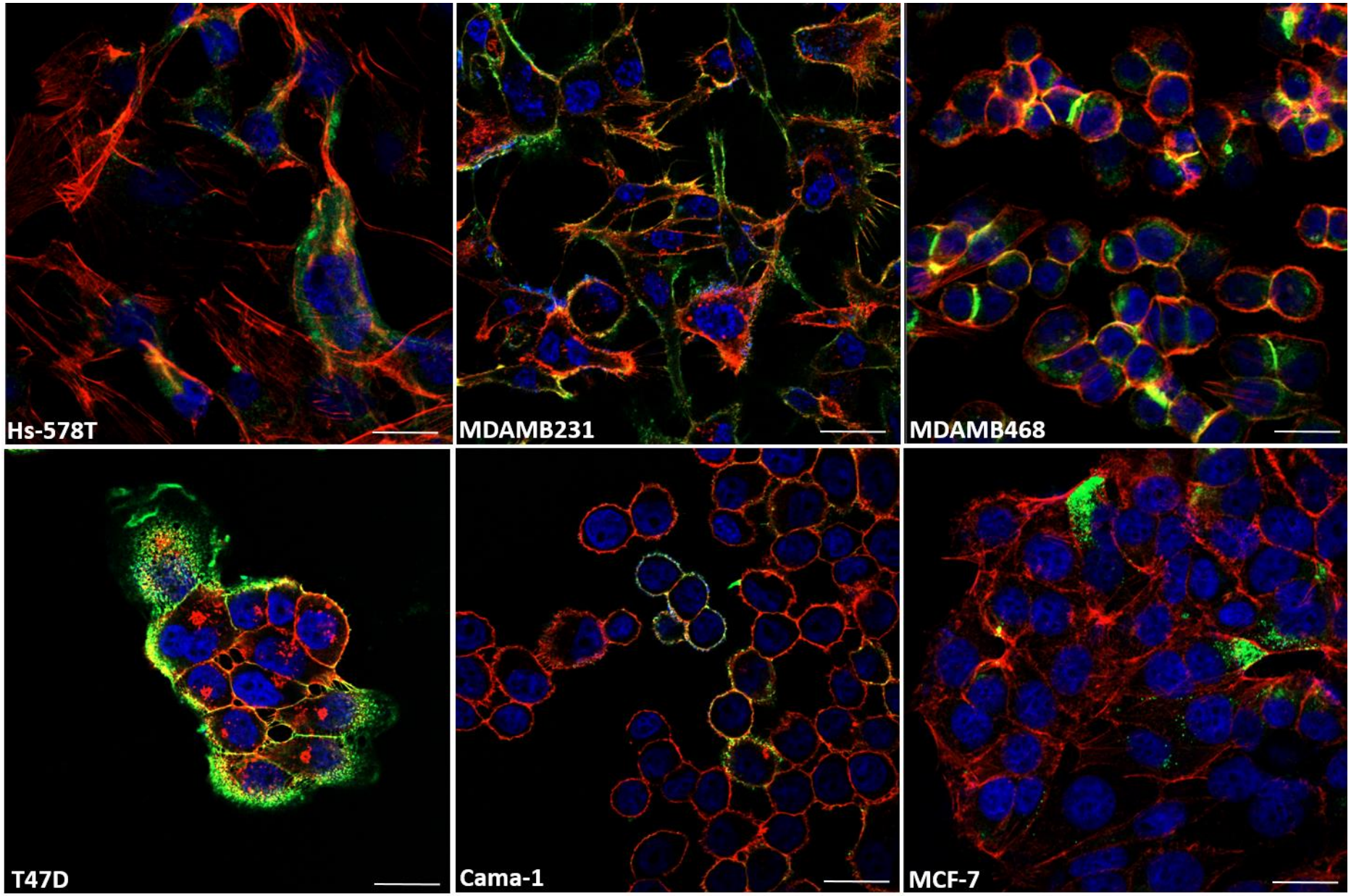

Figure 3

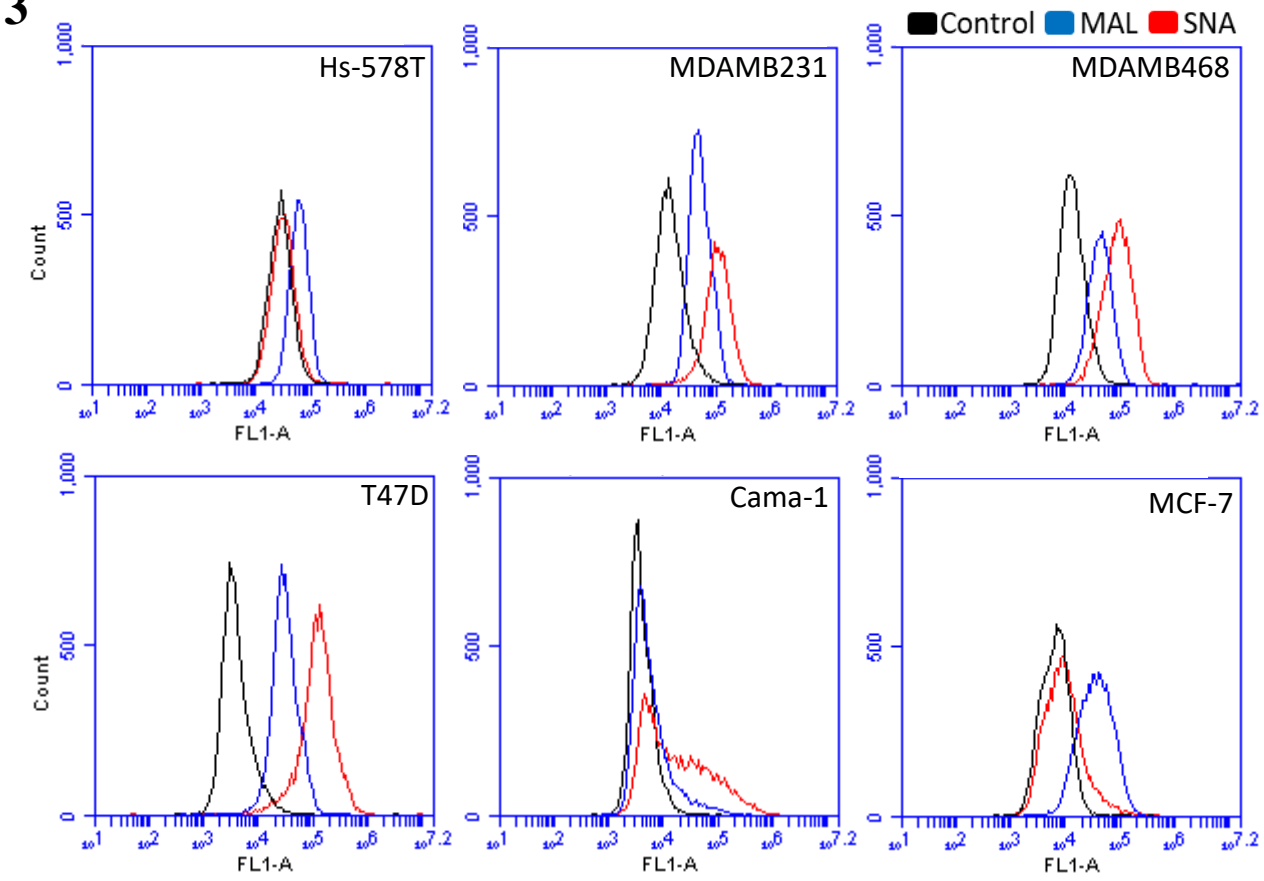
Control
MAL
SNA
Hs-578T
MDAMB231
MDAMB468
T47D
Cama-1
MCF-7
Count
FL1-A
0
500
1,000

Figure 4

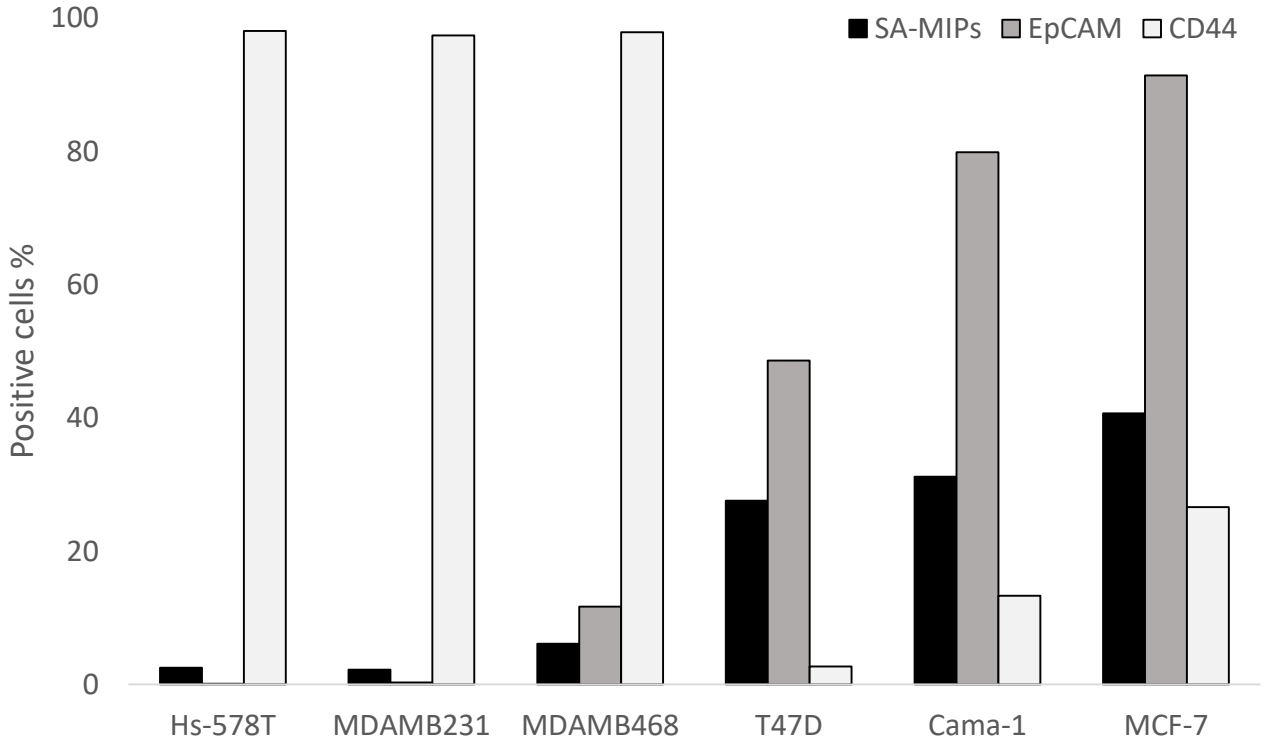

	Hs-578T	MDAMB231	MDAMB468	T47D	Cama-1	MCF-7
SA-MIPs	2,5	2	6,1	27,6	31,2	40,7
EpCAM	0,1	0,3	11,7	48,6	79,9	91,4
CD44	98,1	97,4	97,9	2,7	13,3	26,6

Figure 5

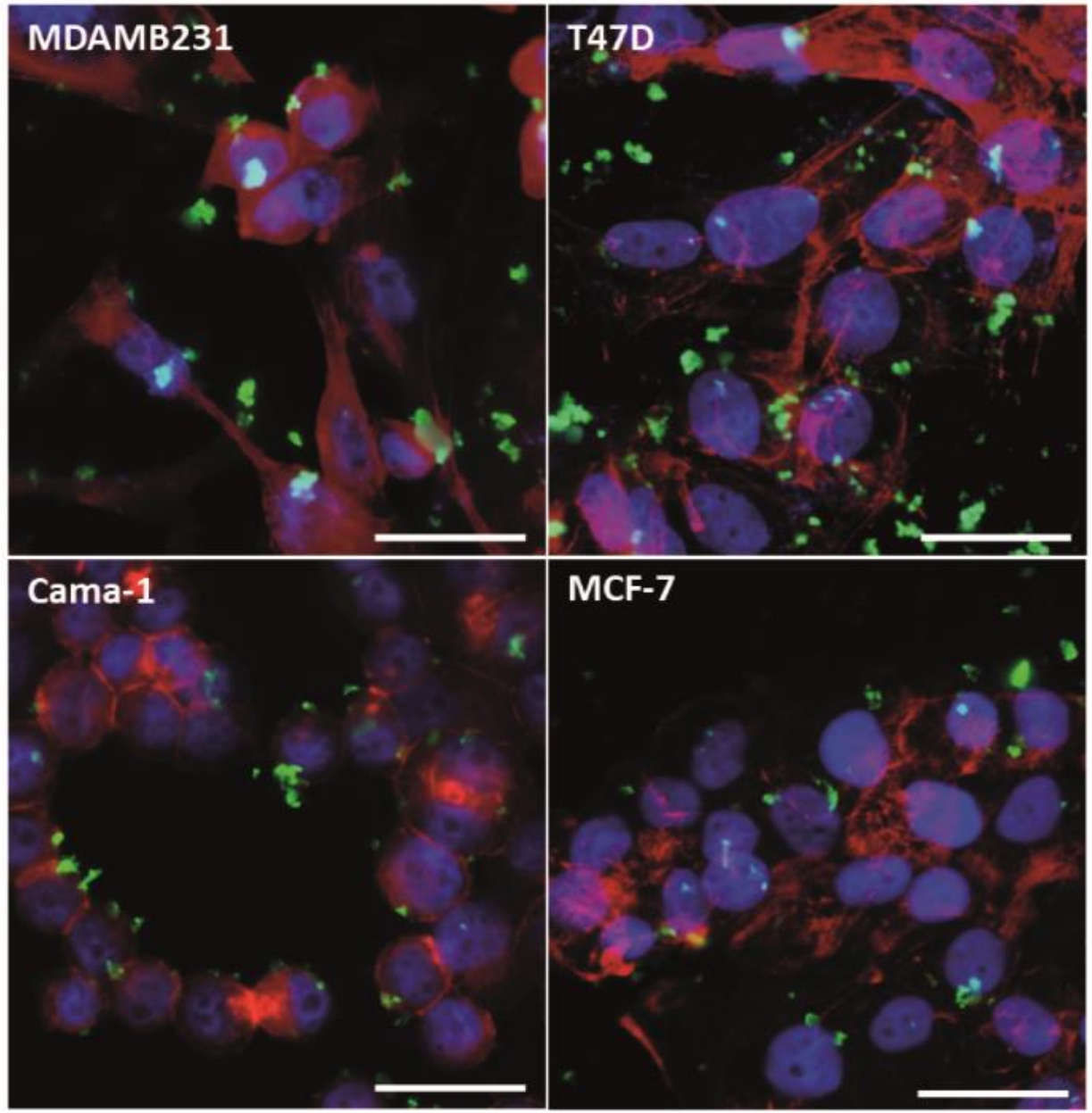

Figure 6

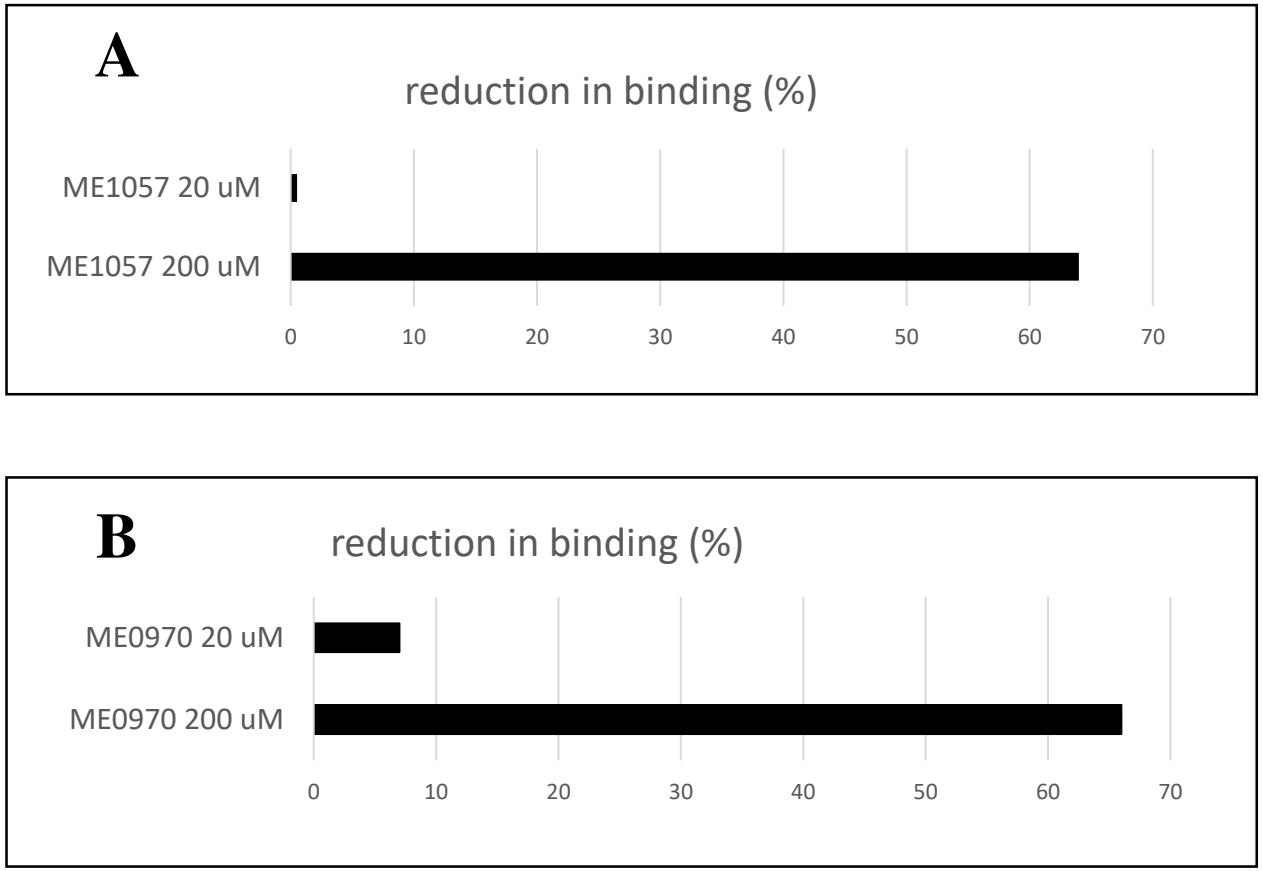
A
reduction in binding (%)
ME1057 20 uM
ME1057 200 uM
0
10
20
30
40
50
60
70
B
reduction in binding (%)
ME0970 20 uM
ME0970 200 uM
0
10
20
30
40
50
60
70

Figures

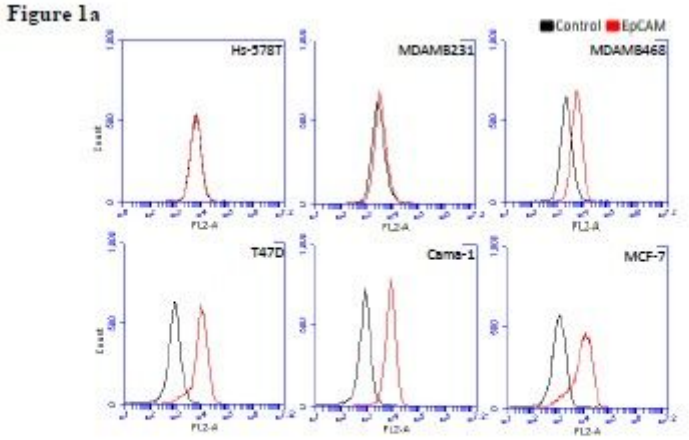

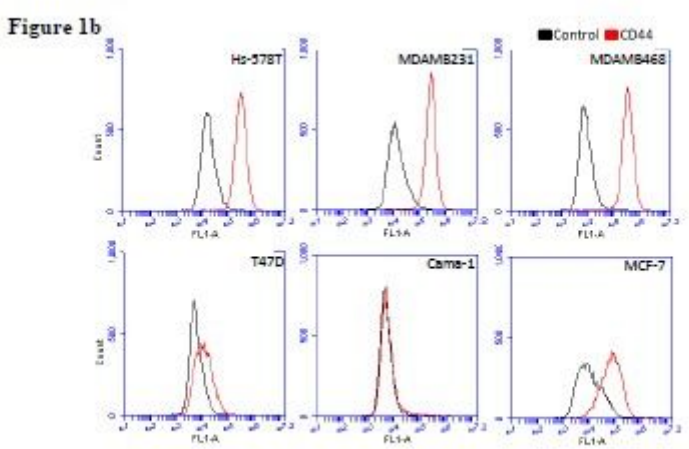

Figure 1

EpCAM and CD44 expression was analyzed with flow cytometry. Six different breast cancer cell lines were analyzed for EpCAM (a) and CD44 (b) expression pattern. The histograms shows the MFI for each staining including background control.

Figure 2a

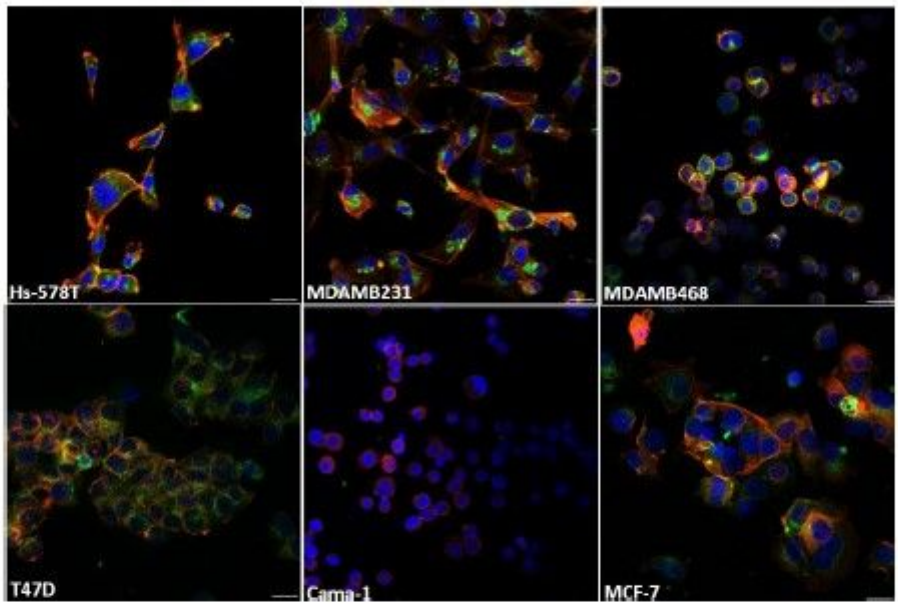

Figure 2b

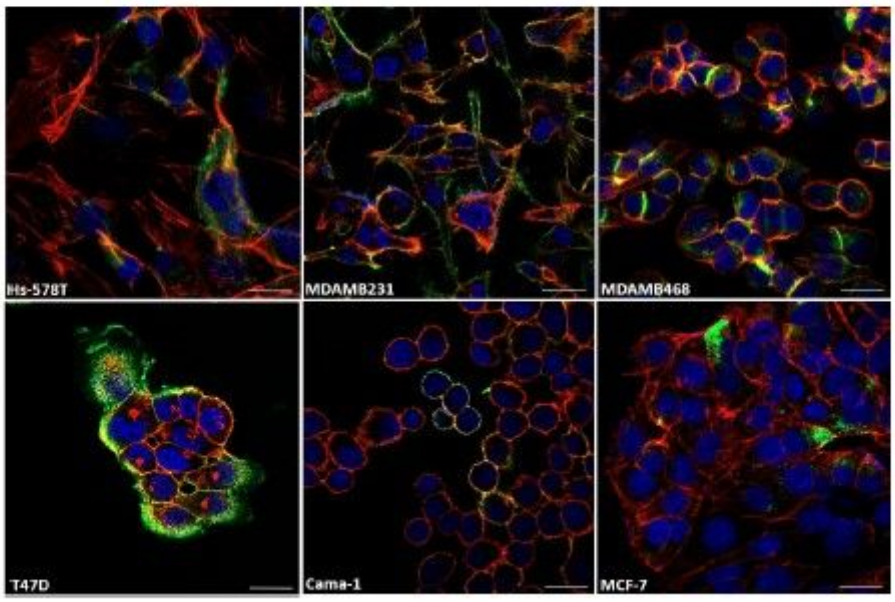

Figure 2

Fluorescence confocal microscopy MAL I - scale bar 20 μm. Six different breast cancer cell lines were stained for MAL I in green, actin filament in red and nuclear in blue, and analyzed with fluorescence microscopy (a). Fluorescence microscopy SNA- scale bar 10 μm. Six different breast cancer cell lines were stained for SNA in green, actin filament in red and nuclear in blue, and analyzed with fluorescence confocal microscopy (b).

Figure 3

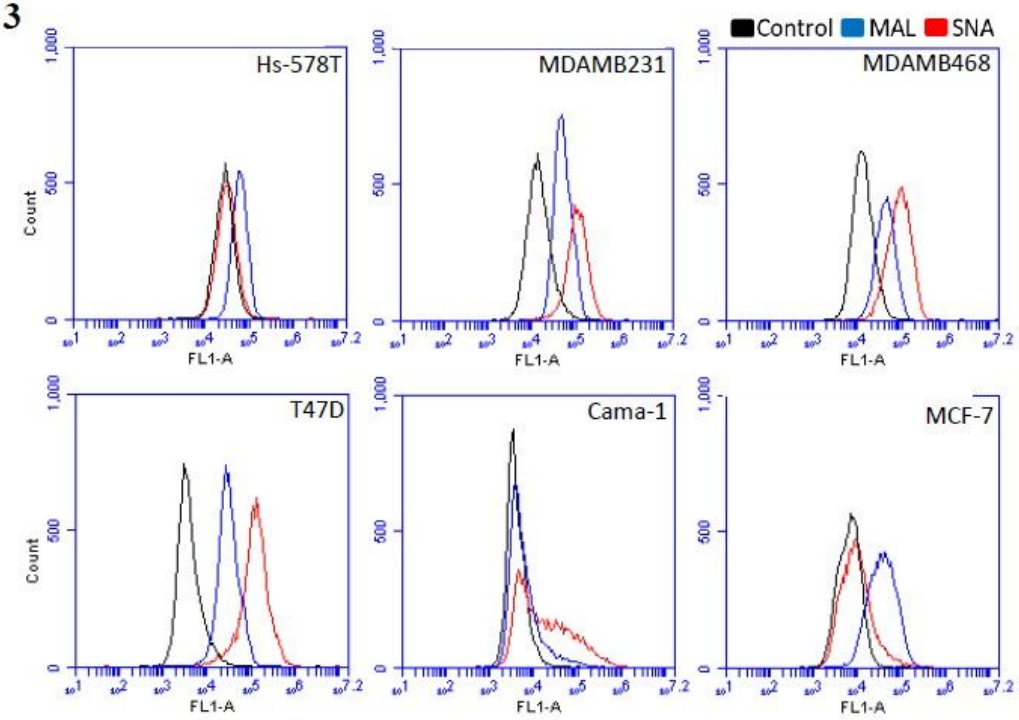

Figure 3

Six breast cancer cell lines were stained with either MAL I or SNA and analyzed with flow cytometry. The histograms shows the MFI for each staining including background control.

Figure 4

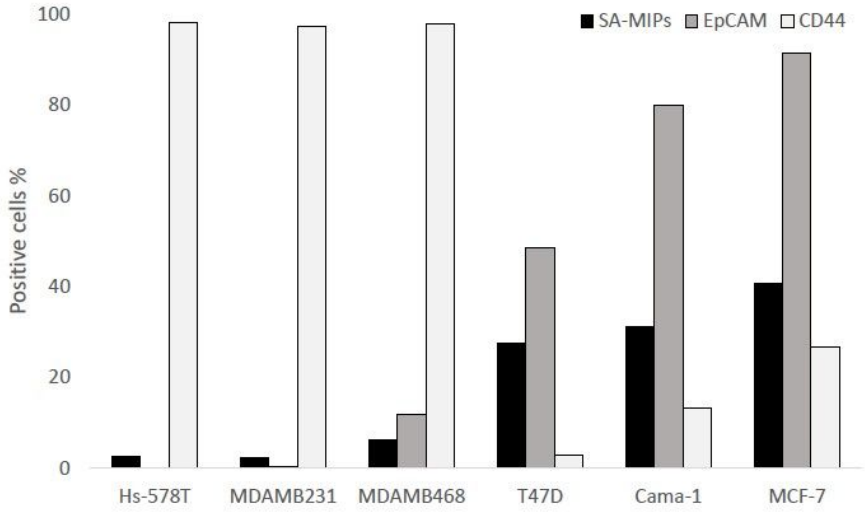

	Hs-578T	MDAMB231	MDAMB468	T47D	Cama-1	MCF-7
SA-MIPs	2,5	2	6,1	27,6	31,2	40,7
EpCAM	0,1	0,3	11,7	48,6	79,9	91,4
CD44	98,1	97,4	97,9	2,7	13,3	26,6

Figure 4

Fluorescence confocal microscopy SA-MIPs - scale bar 20 µm. Four different breast cancer cell lines were stained with SA-MIPs in green, rhodamine-phalloidin (actin filaments) in red and DAPI (nuclei) in blue, and analyzed with fluorescence confocal microscopy.

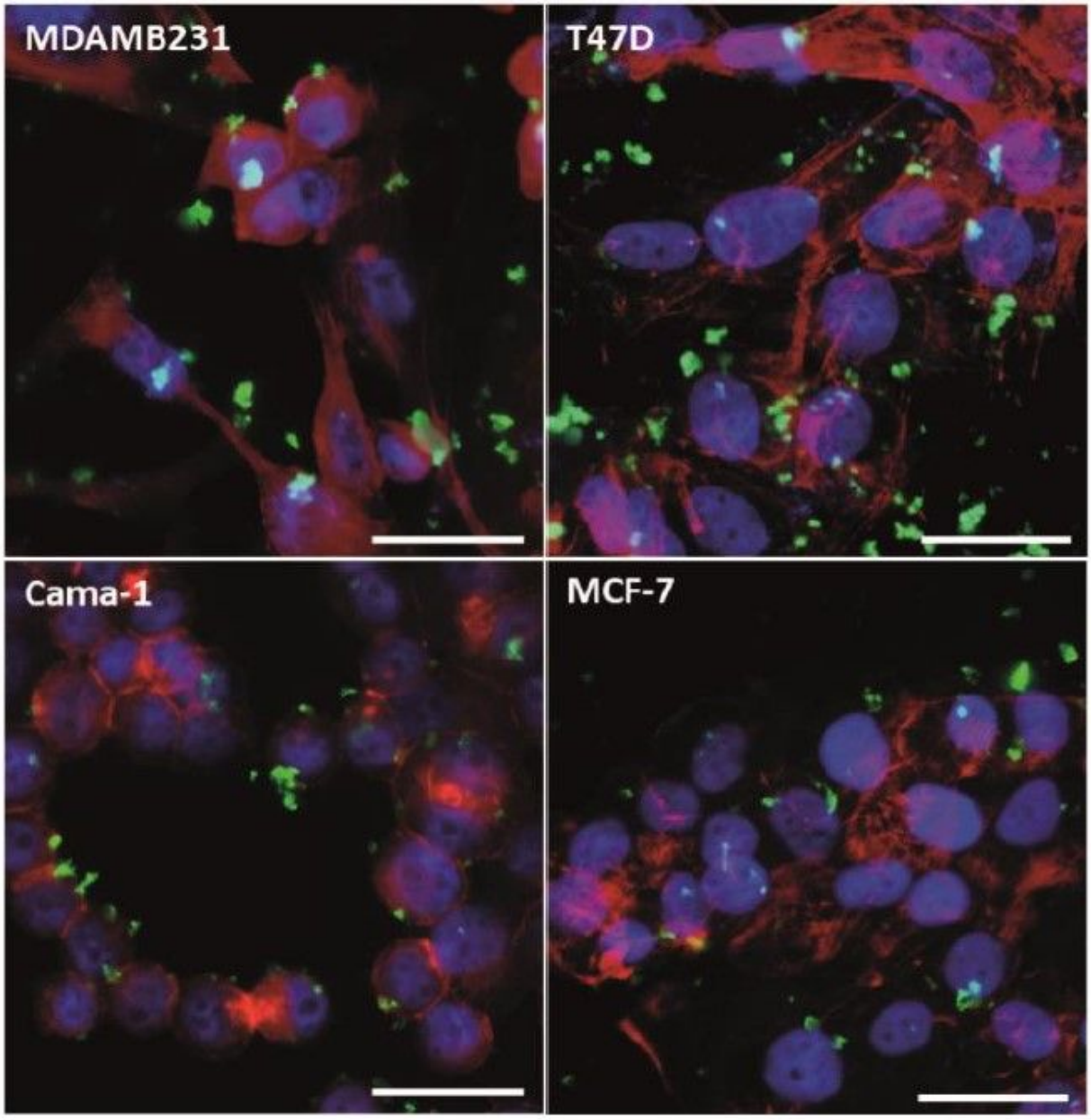

Figure 5

EpCAM, CD44 and SA-MIPs analyzed with flow cytometry. Six different breast cancer cell lines were analyzed for EpCAM, CD44 and SA expression pattern. Results are shown in % positive cells.

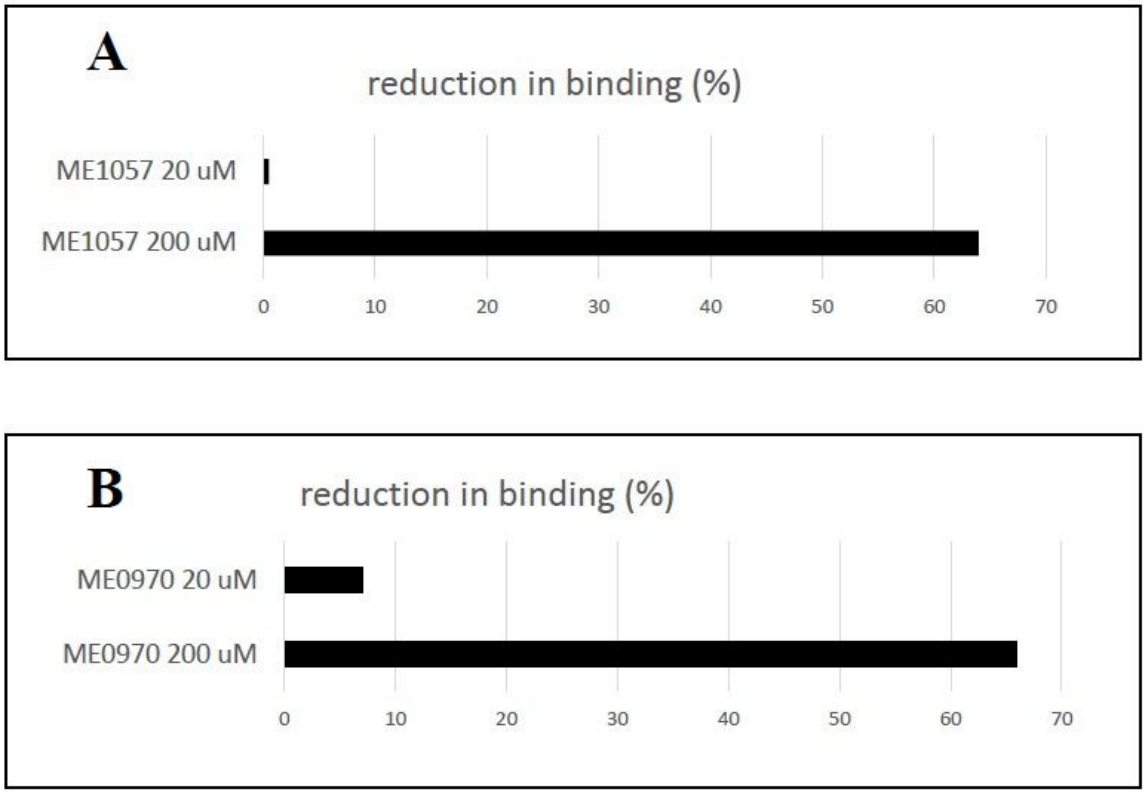

Figure 6

SA-MIPs were pre-incubated with the SA-derivatives ME0970 or ME1057, respectively and analyzed with flow cytometry. The reduction of binding compared to SA-MIP binding alone is shown.